Processes Modulating Calcium Distribution in Citrus Leaves. An Investigation Using X-Ray Microanalysis with Strontium as a Tracer

Richard Storey* and Roger A. Leigh

Horticulture Unit, Commonwealth Scientific and Industrial Research Organisation Plant Industry, Merbein, Victoria 3505, Australia (R.S.); and Department of Plant Sciences, University of Cambridge, Cambridge CB2 3EA, United Kingdom (R.A.L.)

Citrus leaves accumulate large amounts of calcium that must be compartmented effectively to prevent stomatal closure by extracellular Ca^{2+} and interference with Ca^{2+}-based cell signaling pathways. Using x-ray microanalysis, the distribution of calcium between vacuoles in different cell types of leaves of rough lemon (*Citrus jambhiri* Lush.) was investigated. Calcium was accumulated principally in palisade, spongy mesophyll, and crystal-containing idioblast cells. It was low in epidermal and bundle sheath cells. Potassium showed the reverse distribution. Rubidium and strontium were used as tracers to examine the pathways by which potassium and calcium reached these cells. Comparisons of strontium and calcium distribution indicated that strontium is a good tracer for calcium, but rubidium did not mirror the potassium distribution pattern. The amount of strontium accumulated was highest in palisade cells, lowest in bundle sheath and epidermal cells, and intermediate in the spongy mesophyll. Accumulation of strontium in palisade and spongy mesophyll was accompanied by loss of potassium from these cells and its accumulation in the bundle sheath. Strontium moved apoplastically from the xylem to all cell types, and manipulation of water loss from the adaxial leaf surface suggested that diffusion is responsible for strontium movement to this side of the leaf. The results highlight the importance of palisade and spongy mesophyll as repositories for calcium and suggest that calcium distribution between different cell types is the result of differential rates of uptake. This tracer technique can provide important information about the ion uptake and accumulation properties of cells in intact leaves.

Studies of the elemental composition of vacuoles in leaf cells have shown that nutrients are asymmetrically distributed between different cell types (Leigh and Tomos, 1993; Leigh, 2001). This has been studied in most detail in barley (*Hordeum vulgare*), where phosphorus is largely restricted to mesophyll cells, while calcium and chlorine are mainly in epidermal cells, with potassium and nitrate more evenly distributed (Dietz et al., 1992; Leigh and Storey, 1993; Williams et al., 1993; Fricke et al., 1994). Other species also show differences in vacuole composition between different cell types. In wheat, the patterns of distribution are similar to those in barley (Hodson and Sangster, 1988), but in other species they are not. In *Lupinus luteus* leaflets, phosphorus was found at higher concentrations in epidermal cells than in palisade and spongy mesophyll (Treeby et al., 1987), while in sorghum, phosphorus was highest in bundle sheath cells and lowest in the adaxial epidermis, these latter cells containing the highest calcium levels (Boursier and Läuchli, 1989). In the calcicoles, *Centaurea scabiosa* and *Leontodon hispidus*, calcium was highest in palisade, spongy mesophyll, and trichomes, and was excluded from the epidermal cells (De Silva et al., 1996).

Although the physiological reasons for these distributions remain largely unexplained, they do raise questions about their underlying mechanisms and whether they result from differential uptake of ions from the apoplast as the transpiration stream passes different cell types, or whether different ions follow different apoplastic or symplastic pathways from the xylem to particular cell layers (Leigh and Tomos, 1993; Karley et al., 2000b). Attempts to show that different cell types possess different transporters that might differentially remove ions from the transpiration stream have largely been unsuccessful (Dietz et al., 1992; Karley et al., 2000a). Indeed, there is evidence to suggest that the movement of ions to different cell layers cannot be explained fully by assuming ions move in the transpirational water flow from the xylem to the sites of evaporation. In *Commelina communis*, Atkinson (1991) found an even distribution of calcium between adaxial and abaxial epidermal layers even though the rate of transpiration was over 4-fold higher from the abaxial surface. Also, fluorescent dyes fed to cereal leaves via the xylem reach the epidermal layers by traveling along vein extension pathways and appear to bypass the mesophyll (Canny, 1990). These observations suggest that movement of ions through leaves is not always via mass flow in the transpiration stream and that multiple mechanisms may exist to ensure that particular ions move to particular cells (Leigh and Tomos, 1993; Karley et al., 2000b).

* Corresponding author; e-mail richard.storey@csiro.au; fax 61–3–5051–3111.

Article, publication date, and citation information can be found at www.plantphysiol.org/cgi/doi/10.1104/pp.104.045674.

X-ray microanalysis (XRMA) of frozen hydrated tissues (Sigee, 1993) is a powerful method for determining the elemental composition of cells and cell compartments and has been one of the main methods by which differential distribution of nutrients between cells has been investigated (Treeby et al., 1987; Leigh and Storey, 1993; Williams et al., 1993; De Silva et al., 1996; Küpper et al., 2000, 2001; Lombi et al., 2002; Storey et al., 2003). It can be used to measure elemental composition at particular points (e.g. cell compartments or different cells; Leigh et al., 1986; Leigh and Storey, 1993) or to map the distribution of elements within tissues and organs (e.g. Williams et al., 1993). Here we have used both modes to investigate the elemental composition of vacuoles in different cell types in leaves of rough lemon (*Citrus jambhiri* Lush.) and to elucidate the pathways for calcium movement through the leaf using strontium as a tracer. Previous studies have shown that strontium can be used as an analog for calcium in plants (Nelson et al., 1990, and refs. therein), and thus it can be used to label the routes along which calcium travels to reach the cells where it accumulates. Further, there is a lack of discrimination between Ca^{2+} and Sr^{2+} in overall transport from the external medium to the shoot (White, 2001), and voltage-gated Ca^{2+}-permeable channels in plants are also permeable to Sr^{2+} (White et al., 2002). In addition, the H^+/Ca^{2+} antiport at the tonoplast has been reported to show little discrimination between Ca^{2+} and Sr^{2+} (Kim and Heinrich, 1994).

Rough lemon was chosen for these experiments because it is a commercially important citrus rootstock in Australia that, like most citrus rootstocks, permits high levels of calcium accumulation in shoots (Taylor and Dimsey, 1993). Further, citrus leaves may live for up to 2 years and continuously accumulate calcium throughout this period, with concentrations reaching 3% to 6% in dry matter (Robinson et al., 1997). A recent survey showed that only a small number of angiosperms have shoot calcium concentrations greater than 3% (Broadley et al., 2003). Lacking trichomes in which calcium can be accumulated (compare with De Silva et al., 1996), citrus leaves must have efficient mechanisms for compartmenting calcium within other leaf cells to prevent interference with Ca^{2+}-signaling pathways and to avoid stomatal closure induced by extracellular Ca^{2+} (De Silva et al., 1985).

RESULTS

Rough lemon leaves show typical dorsiventral anatomy, with adaxial and abaxial epidermal layers, spongy mesophyll, two layers of palisade mesophyll, and vascular strands surrounded by bundle sheath cells (Fig. 1; see also Esau, 1977). Stomata are only present on the abaxial surface (Schneider, 1968). Just below the adaxial epidermis are large idioblast cells, some of which contain calcium-oxalate crystals. There are also smaller idioblast cells beneath the abaxial epidermis.

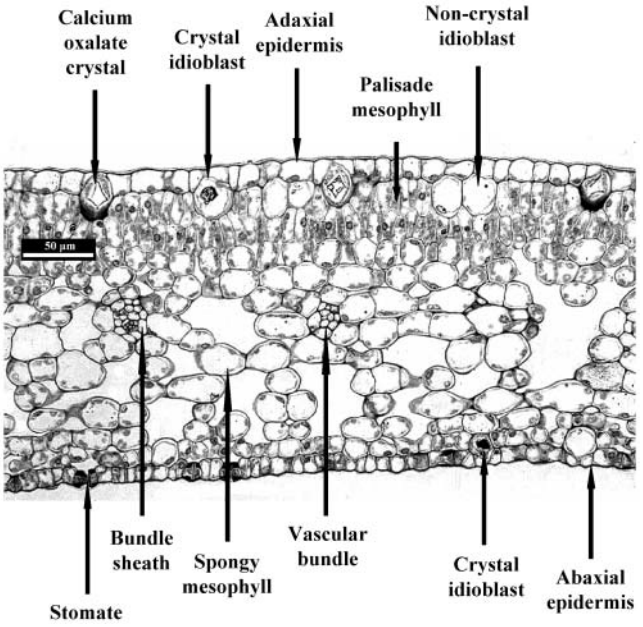

Figure 1. Light micrograph of a transverse section of a rough lemon leaf.

Elemental mapping of the adaxial half of a leaf grown in unamended nutrient solution showed that calcium and potassium were asymmetrically distributed between different cell types (Fig. 2). Calcium was enriched in palisade and spongy mesophyll cells and was also deposited in crystals contained within some idioblast cells (Fig. 2, C and F). These crystal-containing idioblast cells often formed a companion-type arrangement with a crystal-free, potassium-rich idioblast cell (Fig. 2, E and F). Calcium was not accumulated significantly in epidermal or bundle sheath cells. In contrast, potassium was localized mainly in the epidermal cells, bundle sheath, and crystal-free idioblast cells (Fig. 2, B and E), but was much lower in palisade and spongy mesophyll cells.

To quantify these distributions, the (peak − background)/background [(p − b)/b] ratio, a semiquantitative proxy for elemental concentration (Sigee, 1993), was measured for calcium and potassium in vacuoles of the different cell types from young and old leaves. Calcium (p − b)/b ratio was highest in the palisade and spongy mesophyll cells and was low in epidermal cells, particularly in young leaves (Table I). The (p − b)/b ratio for calcium increased 3-fold in the palisade and 2-fold in the spongy mesophyll of older leaves. The highest (p − b)/b values for calcium in vacuoles were considerably less than those measured in calcium-containing crystals in idioblasts that had mean ± SE values of 5.141 ± 0.410 (n = 16). For potassium, the (p − b)/b ratio was highest in adaxial and abaxial epidermal cells and bundle sheath cells. Values were similar in palisade and spongy mesophyll cells in young leaves, but, in older leaves, they were 3-fold higher in the spongy mesophyll than in the palisade

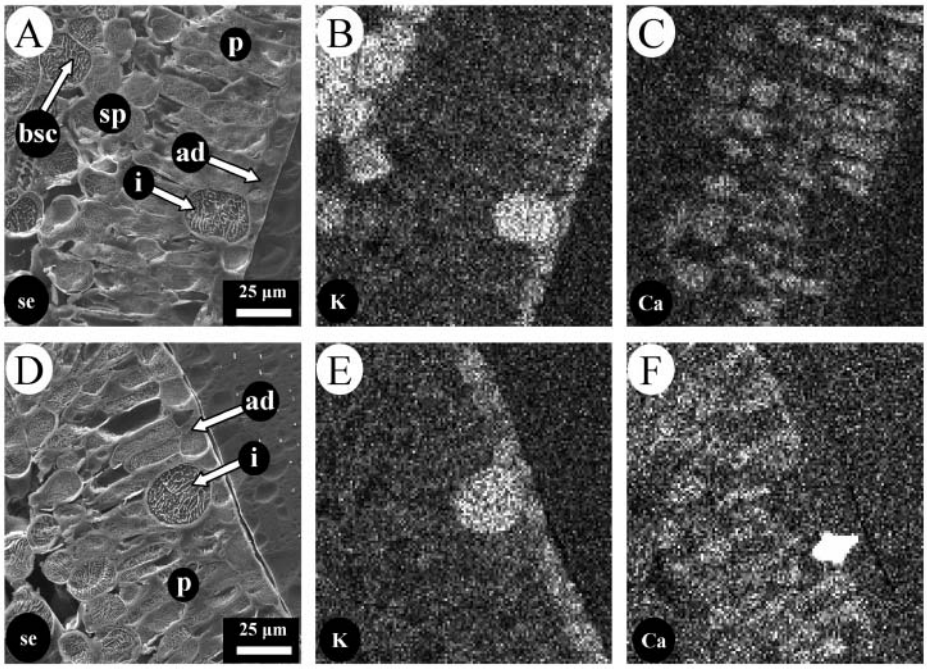

Figure 2. Distribution of potassium and calcium in different cell types in the adaxial half of a leaf from rough lemon grown in unamended nutrient solution. A and D, Secondary electron images; B and E, potassium distribution; C and F, calcium distribution. A to C and D to F are from different leaves. ad, Adaxial epidermis; bsc, bundle sheath cell; i, idioblast cell; p, palisade mesophyll; sp, spongy mesophyll.

mesophyll. The potassium (p − b)/b ratio in bundle sheath cells increased by about 50% in older leaves. Plots of the relationship between the (p − b)/b ratios for potassium and calcium in each of the cell types showed that cells with high calcium (e.g. palisade mesophyll) generally had low potassium, while the reverse was observed for other cells (e.g. bundle sheath and noncrystal idioblasts; Fig. 3A). The exception was spongy mesophyll, which had a wide range of concentrations of both elements, although this appeared to be related to the position of the cells in the leaf, with those immediately beneath the abaxial epidermis having more calcium than those deeper within the lamina (Fig. 3B).

To investigate the pathways by which calcium and potassium reached their final locations in epidermal and mesophyll cells, the possibility of using strontium and rubidium as tracers for calcium and potassium, respectively, was investigated by feeding these to excised transpiring leaves through their petioles. After just 4 h, rubidium was found in all cell types and did not show the cell-specific distribution observed for potassium (compare Fig. 4, B and C). However, after a similar labeling period, strontium mimicked the distribution of calcium and was present in vacuoles of both types of mesophyll cells but not in epidermal cells (Fig. 4, G and H). Unlike the endogenous calcium, it accumulated in the periclinal and tangential cell walls

Table I. *Distributions of potassium and calcium, measured as (p − b)/b ratios, in different leaf cell types of young and old leaves from rough lemon grown in unamended nutrient solution*

Cell Type	(p − b)/b			
	Potassium		Calcium	
	Young[a]	Old[a]	Young	Old
Adaxial epidermis	0.332 ± 0.018[b]	0.387 ± 0.026	0.013 ± 0.003	0.054 ± 0.006
Palisade mesophyll	0.109 ± 0.010	0.120 ± 0.010	0.133 ± 0.008	0.390 ± 0.020
Spongy mesophyll	0.094 ± 0.015	0.356 ± 0.026	0.112 ± 0.010	0.234 ± 0.024
Bundle sheath	0.382 ± 0.019	0.570 ± 0.014	0.013 ± 0.002	0.017 ± 0.003
Abaxial epidermis	0.285 ± 0.019	0.368 ± 0.021	0.017 ± 0.002	0.039 ± 0.004

[a]The young leaf was almost fully expanded and the old leaf was taken from the 17th node distal to the young leaf. [b]Data are presented as mean ± SE (n = 10 cells of each cell type from a single leaf of each age). The LSDs (at P = 0.05) were: for potassium, cell type = 0.040; age = 0.025; cell type × age = 0.056; for calcium, cell type = 0.025; age = 0.016; cell type × age = 0.036.

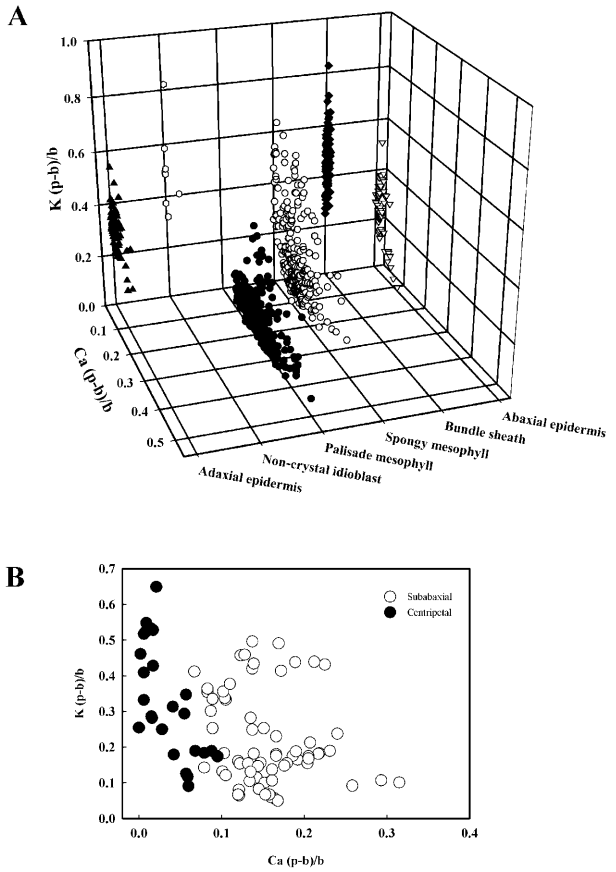

Figure 3. The relationship between vacuolar (p − b)/b ratios for potassium and calcium of different cell types in leaves from rough lemon grown in unamended nutrient solution. A, All cell types (892 cells from 24 leaves); B, spongy mesophyll cells either adjacent to the abaxial epidermis (subabaxial) or near the vascular bundles (centripetal) within the abaxial half of the lamina (95 cells from 4 leaves).

of the adaxial epidermal cells. Other experiments (not shown) demonstrated that calcium also accumulated in the adaxial epidermal cell walls when fed to excised leaves through their petioles, confirming that strontium faithfully reports the distribution pathways for calcium. A more detailed investigation based on (p − b)/b ratios in vacuoles of different cell types confirmed that, following uptake for 24 h from a solution containing 25 mM $SrCl_2$, strontium was found mostly in the palisade and spongy mesophyll cells of the leaf and was notably low in bundle sheath and crystal-free idioblast cells (Table II). In these leaves, which were grown in low Cl^-, the Cl^- counter anion was more evenly distributed than strontium between the different cell types (Table II). This general distribution of chlorine was also observed in the experiment with RbCl (Fig. 4D).

To confirm that the distribution of strontium was mirroring that of calcium, excised leaves from plants with low leaf calcium concentrations (achieved by growth in nutrient solution containing 50 mM KCl) were fed 25 mM $Sr(NO_3)_2$ and 25 mM $Ca(NO_3)_2$ for 24 h, and the (p − b)/b ratios for strontium and calcium were compared in vacuoles of the different cell types. Palisade and spongy mesophyll cells from low-calcium plants had (p − b)/b ratios for calcium of 0.047 ± 0.003 and 0.022 ± 0.004 (mean ± SE), respectively, compared with equivalent values of 0.277 ± 0.013 and 0.149 ± 0.007 in cells from leaves of plants grown in unamended nutrient solution without additional KCl (n = 10–15 cells from one leaf, in all cases). The subsequent uptake of calcium and strontium by the low-calcium leaves led to the differential accumulation of these elements in different cells. Bundle sheath cells accumulated the least and palisade mesophyll the most, other cell types being intermediate (Fig. 5). After 24 h, the (p − b)/b ratios for calcium in the palisade and spongy mesophyll cells were raised significantly above those in low-calcium leaves and were approaching those measured in high-calcium leaves grown throughout their life in unamended nutrient solution (Fig. 5; compare with Table I). The levels of calcium and strontium in all cells were highly correlated over a range of (p − b)/b ratios from 0 to approximately 0.3, with all points falling on or close to the regression line (Fig. 5). The (p − b)/b ratios plotted in Figure 5 were adjusted to allow for the different sensitivities of XRMA to calcium and strontium (see "Materials and Methods"), so the slope of approximately 1 for the regression line indicates that there was equimolar accumulation of both calcium and strontium. This suggests that strontium distributes to the vacuoles of different cells in the same way as calcium, confirming its value as a tracer for calcium in citrus leaves.

Mapping experiments showed that strontium accumulated in the apoplast around epidermal cells, so movement through cell walls is probably the main route by which strontium, and by implication calcium, moves from the xylem to the different cell types, where it accumulates (Fig. 4H). Thus, more detailed surveys of strontium localization were undertaken (Fig. 4, I–R). After 24-h uptake from a solution of 50 mM $Sr(NO_3)_2$ and 5 mM KCl, the strontium signal was strong from regions within the vascular bundle (presumably xylem vessels) and cell walls in the bundle sheath (Fig. 4K), particularly at the apex of the intercellular junctions (arrows in Fig. 4K). There was no significant accumulation of strontium in vacuoles in this region, which were high in potassium (Fig. 4J; compare with Fig. 2B). Strontium could also be detected in the apoplast of palisade mesophyll cells, but this depended on the calcium status of the leaves. It was detected around these cells in low-calcium leaves but not in high-calcium leaves (compare Fig. 4, M and O), even though in both cases it was present in the apoplast of the adjacent adaxial epidermal cells. Strontium also accumulated in the cell walls of noncrystal and crystal idioblast cells, clearly being incorporated into the crystals of the latter (Fig. 4, P–R).

The presence of strontium in the apoplast of adaxial epidermal cells more distant from the xylem than the

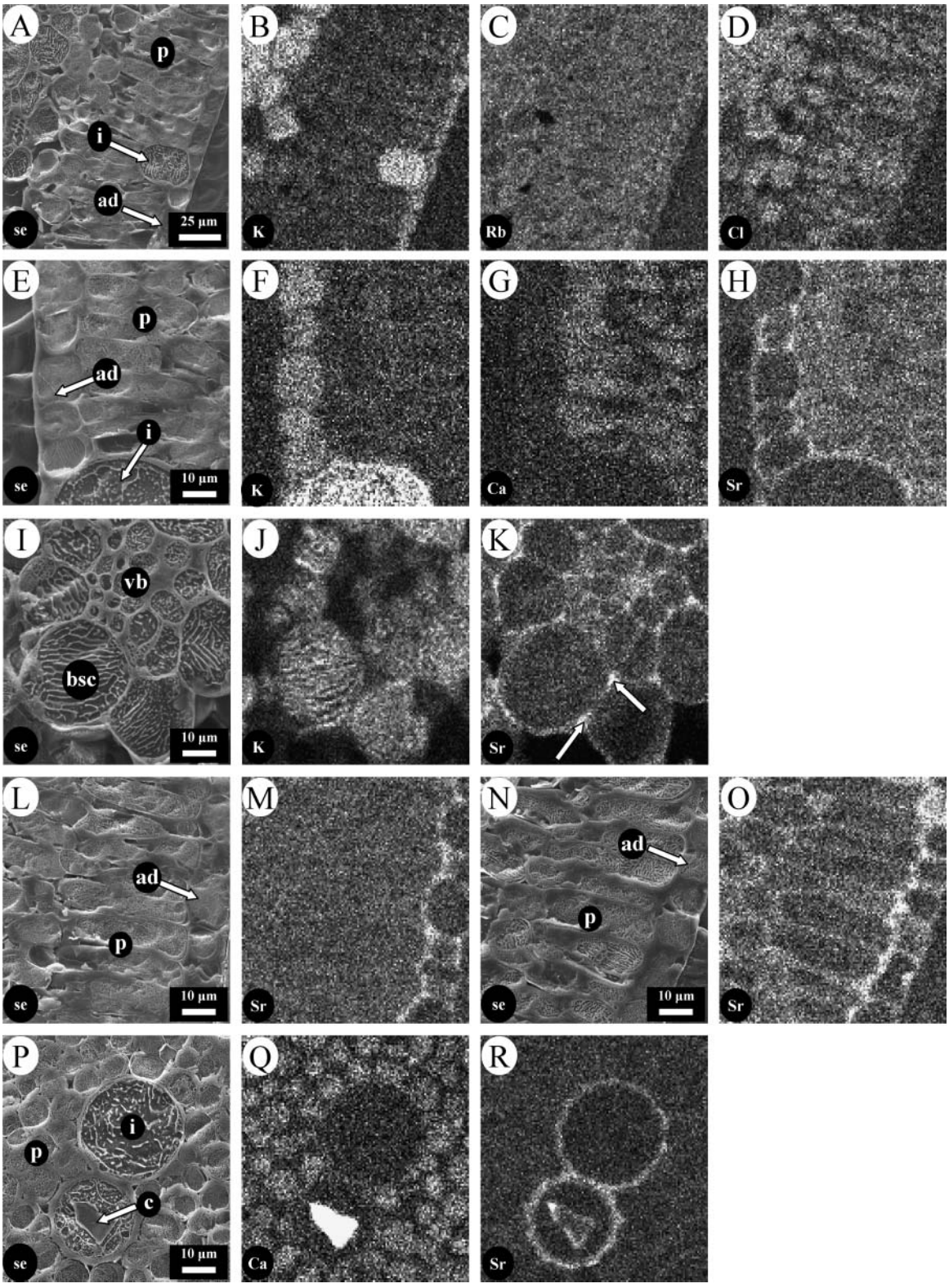

Figure 4. Elemental distributions in excised leaves of rough lemon after uptake of rubidium and strontium tracers. Unless otherwise stated, plants were grown in unamended nutrient solution. A to D, Uptake from 25 mM RbCl for 4 h. A, Secondary electron image; B, potassium distribution; C, rubidium distribution; D, chlorine distribution. E to H, Uptake from 50 mM $Sr(NO_3)_2$ for 4 h. E, Secondary electron image; F, potassium distribution; G, calcium distribution, H, strontium distribution. I to K, Area around the vascular bundle after uptake of 50 mM $Sr(NO_3)_2$ for 24 h. I, Secondary electron image. J, potassium distribution; K, strontium distribution. L to O, Uptake from 50 mM $Sr(NO_3)_2$ for 4 h by a high-calcium leaf (L and M) and a low-calcium leaf (N and O). L and N, Secondary electron images; M and O, strontium distribution. P to R, Pair of idioblast cells after uptake from 50 mM $Sr(NO_3)_2$ for 4 h. P, Secondary electron image; Q, calcium distribution; R, strontium distribution. c, Crystal; vb, vascular bundle; other abbreviations as in legend to Figure 2.

Table II. *Distributions of potassium, calcium, strontium, and chlorine, measured as (p − b)/b ratios, in different cell types of an excised leaf from rough lemon grown in unamended nutrient solution and fed 25 mM $Sr(Cl)_2$ + 5 mM KCl through its petiole for 24 h*

Cell Type	(p − b)/b			
	Potassium	Calcium	Strontium	Chlorine
Adaxial epidermis	0.334 ± 0.008[a]	0.023 ± 0.002	0.051 ± 0.006	0.118 ± 0.004
Palisade mesophyll	0.066 ± 0.008	0.164 ± 0.006	0.256 ± 0.006	0.208 ± 0.009
Spongy mesophyll	0.105 ± 0.013	0.144 ± 0.014	0.196 ± 0.013	0.239 ± 0.009
Bundle sheath	0.390 ± 0.032	0.012 ± 0.003	0.013 ± 0.005	0.171 ± 0.009
Noncrystal idioblast	0.571 ± 0.097	0.007 ± 0.004	0.004 ± 0.002	0.157 ± 0.037
Abaxial epidermis	0.254 ± 0.025	0.008 ± 0.003	0.039 ± 0.011	0.138 ± 0.011

[a]Data are presented as mean ± SE (n = 3 to 10 cells of each type from one leaf). The LSDs (at P = 0.05) between cell types were: potassium, 0.078; calcium, 0.032; strontium, 0.031; chlorine, 0.038.

palisade cells, but not always in the cell walls of the latter, seems contradictory because, if strontium moves extracellularly, it must pass through the palisade apoplast to reach the adaxial epidermis. This effect is probably explained by the rate at which strontium is taken up by palisade cells in high- and low-calcium leaves. After 4 h of loading with 50 mM $Sr(NO_3)_2$, the (p−b)/b ratio for strontium in vacuoles of palisade cells in low-calcium leaves was only one-third that in high-calcium leaves (Table III), but, after 24 h, the values were similar. In high-calcium leaves, the extra 20 h of loading only doubled the strontium (p − b)/b ratio in palisade cells, but raised it 7-fold in low-calcium leaves. Thus, there was a large difference in the amount of strontium accumulated in cells of high- and low-calcium leaves at 4 h, but not at 24 h. Any strontium that is not taken up into palisade cells accumulates around the adjacent adaxial epidermal cells, which do not accumulate significant amounts of strontium (Tables II and III; Fig. 5). Initial accumulation of strontium in spongy mesophyll cells was also related to calcium status, but the (p − b)/b ratios were much smaller than in the palisade cells (Table III; Fig. 5).

There was a more-or-less equal movement of strontium into the adaxial and abaxial halves of the leaf. Using a beam voltage of 25 kV to ensure good penetration beneath the surface of an intact piece of leaf, the (p − b)/b ratios for strontium were measured at the adaxial and abaxial sides of leaves. After a 2-h uptake from 25 mM strontium, (p − b)/b ratios of 0.074 and 0.072 were measured at the adaxial and abaxial sides, respectively. A similar treatment with 50 mM strontium gave values of 0.128 and 0.118. Thus, in transpiring excised leaves, strontium was uniformly distributed between the two transverse halves of the leaf, even though the bulk of transpiration must be through the abaxial surface, which contains all of the stomates (Fig. 1). The presence of significant strontium levels in the apoplast of the adaxial half of the leaf (see Fig. 4) suggested that cuticular water loss might be sufficiently high to account for some or all of the strontium movement to this surface. To test this hypothesis, the adaxial leaf surface of one longitudinal half of a leaf was covered with Vaseline (Lever-Rexona, North Rocks, Australia), with the other half acting as an untreated control. Strontium distribution was analyzed after uptake from 25 mM $Sr(Cl)_2$ for 24 h. There was little difference in the accumulation of strontium at the adaxial surface in the two halves of the leaf. Comparison of (p − b)/b ratios for strontium at this surface gave mean ± SE values of 0.228 ± 0.005 in the untreated half, and 0.213 ± 0.005 in the treated half (20 measurements on a single leaf in both cases); this 7% decrease was, however, significant at P = 0.05. Mapping showed that the strontium was present in the apoplast of both the adaxial and abaxial epidermal cells in both treatments (not shown).

Covering half of the abaxial surface of a leaf with Vaseline completely prevented strontium accumulation in the treated half, presumably because transpiration was abolished and this stopped xylem transport

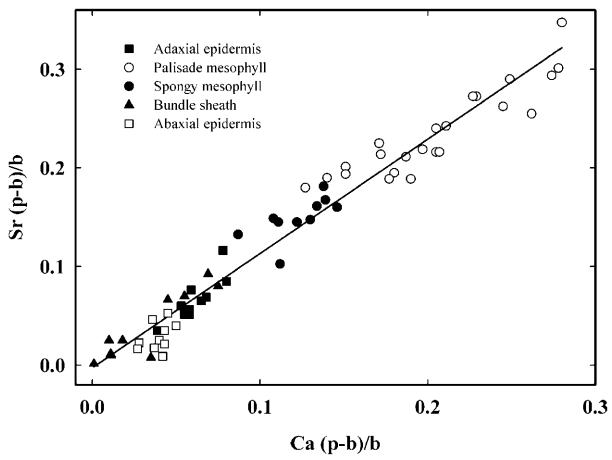

Figure 5. Relationship between vacuolar (p − b)/b ratios for calcium and strontium of different cell types in an excised leaf from rough lemon grown under low-calcium conditions and fed 25 mM $Sr(NO_3)_2$ and 25 mM $Ca(NO_3)_2$ through its petiole for 24 h. Results from 65 cells in one leaf. Values of (p − b)/b ratios were adjusted for the different sensitivities of the XRMA to calcium and strontium, so the slope of the line reflects the molar accumulation ratio of the two elements (see "Materials and Methods"). The fitted regression line is shown ($y = 1.16x - 0.003$; $r^2 = 0.962$).

Table III. *Effect of leaf calcium status on the distribution of strontium between different cell types after uptake from 50 mM $Sr(NO_3)_2$ + 5 mM KCl for 4 or 24 h*

Cell Type	Strontium (p − b)/b			
	4 h		24 h	
	High Calcium[a]	Low Calcium[b]	High Calcium	Low Calcium
Adaxial epidermis	0.017 ± 0.002[c]	0.003 ± 0.002	0.032 ± 0.006	0.042 ± 0.007
Palisade mesophyll	0.089 ± 0.007	0.031 ± 0.005	0.196 ± 0.007	0.208 ± 0.016
Spongy mesophyll	0.061 ± 0.005	0.008 ± 0.003	0.048 ± 0.007	0.047 ± 0.014
Abaxial epidermis	0.006 ± 0.003	0.014 ± 0.004	0.036 ± 0.003	0.049 ± 0.006

[a]From a plant grown in unamended nutrient solution. [b]From a plant grown in nutrient solution containing 50 mM KCl. [c]Data are presented as mean ± SE (n = 5–10 for each cell type in a single leaf from each treatment). The LSDs (at $P = 0.05$) were: for 4-h uptake, cell type, 0.011; age, 0.008; cell type × calcium status, 0.016; for 24-h uptake, cell type, 0.018; age, not significant; cell type × calcium status, not significant.

of strontium to that half of the leaf. However, strontium still accumulated in the untreated half, and this allowed an investigation of whether strontium accumulation in palisade and spongy mesophyll affected the levels of other elements. After uptake from 25 mM $Sr(Cl)_2$ for 24 h, the differences in (p − b)/b ratios for elements in cells in the Vaseline-treated and -untreated halves of the leaves were determined. The untreated half of the leaf showed a net increase of strontium in palisade and spongy mesophyll cells, but not in adaxial epidermal or bundle sheath cells (Fig. 6). The increases in strontium in the palisade and spongy mesophyll cells were accompanied by a decrease in potassium levels in both cell types and an increase in the bundle sheath cells. Strontium accumulation was accompanied by small elevations in vacuolar calcium in palisade and spongy mesophyll cells, while chlorine accumulated in all cell types, as observed in other experiments.

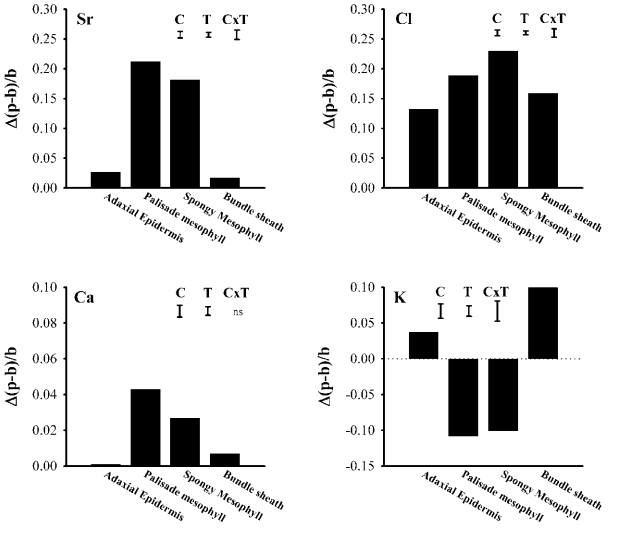

Figure 6. Differences in vacuolar (p − b)/b ratios for strontium, chlorine, calcium, and potassium between cells in the transpiring and nontranspiring halves of an excised leaf from rough lemon grown in unamended nutrient solution and fed 50 mM $Sr(Cl)_2$ through its petiole for 24 h. Transpiration in one longitudinal half of the leaf was prevented by covering the abaxial surface with Vaseline; the other half was left untreated. Positive numbers indicate that the (p − b)/b ratio was higher in cells of the untreated, transpiring half of the leaf; negative numbers indicate that they were smaller. Results from 140 cells in one leaf. Capped bars indicate LSDs ($P = 0.05$) between cells (C), treatments (T), and cells × treatment interaction (C × T).

DISCUSSION

Calcium is asymmetrically distributed between different cell types in leaves of rough lemon. It accumulates in much higher concentrations in palisade and spongy mesophyll cells than in epidermal cells, and is deposited as crystals in idioblast cells (Fig. 1; Table I). This pattern is distinct from that for potassium and is not affected by leaf age even though calcium levels rise with leaf age (Table I). In general, cells of any particular type in rough lemon leaves all behave similarly and accumulate either high calcium and low potassium or vice versa, suggesting they are selective in the cations they absorb (Fig. 3A). Spongy mesophyll cells are an exception and have a wide range of both calcium and potassium concentrations, possibly related to their position in the leaf (Fig. 3B). Similar enrichment of calcium in palisade and spongy mesophyll cells, but not in epidermal cells, has been seen in other species, including the metal hyperaccumulators *Alyssum lesbiacum*, *Alyssum bertolonii*, *Thlaspi geosingense*, and *Arabidopsis halleri* (Küpper et al., 2000, 2001), the calcicoles *C. scabiosa* and *L. hispidus* (De Silva et al., 1996), the calcifuge *L. luteus* (De Silva and Mansfield, 1994), and the fern *Pteris vittata* (Lombi et al., 2002). This pattern of calcium distribution is quite distinct from that seen in cereals, where calcium is enriched in the epidermis (Leigh and Tomos, 1993, and refs. therein). In cereals, it was speculated that calcium was accumulated in the epidermis to separate it spatially from phosphorus, which was enriched in vacuoles of mesophyll cells, thereby preventing formation of insoluble $CaHPO_4$ (Leigh and Storey, 1993). Accumulation of high calcium in the vacuoles of

palisade and spongy mesophyll cells of citrus and the other species mentioned above would be incompatible with a vacuolar storage of inorganic phosphate in these cells. Measurements in *L. luteus* suggest that spatial separation of calcium and phosphorus still occurs in these species that accumulate calcium in palisade and spongy mesophyll cells because, in this plant, phosphorus is located in epidermal cells, not in palisade or spongy mesophyll (Treeby et al., 1987). The chemical state of calcium in palisade and spongy mesophyll cells of rough lemon is unclear. We found no indication of particulate calcium in these cells that would indicate the presence of calcium oxalate. Even when present as crystal sand, the calcium oxalate particles can be up to 5 μm in length (Levy-Lior et al., 2003), well within the resolution of mapping. The absence of detectable crystals in the mesophyll cells contrasts with the obvious inclusions in crystal idioblasts (Figs. 2 and 4). We conclude that it is unlikely that there is crystalline calcium oxalate in the palisade and spongy mesophyll of rough lemon, but this must be confirmed by other means.

It is clear from the distribution of calcium and potassium in citrus that their accumulation in particular cell types is not related to the position of cells along the likely path of the transpiration stream through the leaf. Thus, even though the palisade and spongy mesophyll lie between the vascular bundles and the leaf surfaces, they accumulate more calcium than the bundle sheath or epidermal cells. The reverse is true for potassium. This selectivity could arise either because the transport properties of each cell type allow them to absorb only particular nutrients from the transpiration stream, or because each nutrient element moves along a different pathway in the leaf and so is only available to certain cell types (Leigh and Tomos, 1993; Karley et al., 2000b). To investigate which of these possibilities might apply to calcium, we used strontium as a tracer. Strontium has previously been shown to be a good tracer for calcium (Nelson et al., 1990; Kim and Heinrich, 1995; Gierth et al., 1998) and is also taken up into calcium-oxalate crystals in idioblast cells (e.g. Franceschi and Schueren, 1986; Kim and Heinrich, 1995). In citrus leaves, calcium and strontium were accumulated in parallel in all cell types when fed to leaves grown under conditions that gave rise to low-calcium cells (Fig. 5). The strong correlation between the levels of calcium and strontium indicates that the cells do not discriminate strongly between the two elements and confirms the utility of strontium as a tracer for calcium in this system. Further, strontium distributed itself in the same way as calcium. Thus, it accumulated to low concentrations in bundle sheath and epidermal cells, to intermediate concentrations in spongy mesophyll, and to highest concentrations in palisade cells, exactly mirroring the way calcium was distributed (Figs. 2 and 5). This differential accumulation of strontium contrasts with the more general distributions of rubidium and Cl^- when these were fed to leaves (Figs. 4 and 6; Table II).

After short- and long-term loading, high concentrations of strontium and calcium were detectable in the apoplast around all major cell types (Fig. 4 for strontium; calcium data not shown), indicating that the apoplast is the main pathway for strontium and calcium distribution in the leaf. After just 4 h, strontium was detectable within palisade cells (Fig. 4H) and was incorporated into calcium-oxalate crystals in idioblast cells (Fig. 4R), but was not detectable within adjacent adaxial epidermal cells even though these had high concentrations of strontium in their cell walls (e.g. Fig. 4, H, M, and O). Thus, although all cells in the leaf were exposed to strontium, it accumulated only in some, indicating that the observed distribution between different cells results from differential uptake, not differential rates of supply. Further, the constancy of the ratio between strontium and calcium in different cell types (Fig. 5) indicates that the transport systems in each of the different cells do not discriminate strongly between these two ions. This suggests that the underlying transport mechanisms are the same in all cells, but their capacity differs in each cell type, and this is what leads to differential accumulation. The strontium/calcium accumulation measured here is in the vacuole, and the data do not allow any conclusion about whether the transport systems that give rise to the cellular differences in strontium/calcium accumulation are located at the plasma membrane or tonoplast. The amount of each element accumulated in the vacuole must be a balance between influx and efflux processes at the plasma membrane and tonoplast. The final accumulation ratios will be the combined result of transport via ion channels, H^+-linked cotransporters, and Ca^{2+}-ATPases, each with a different selectivity for Ca^{2+} and Sr^{2+} (White, 2001; White et al., 2002; White and Broadley, 2003). The observation that cells in high-calcium leaves initially took up strontium more rapidly than those in low-calcium leaves (Table III) suggests calcium-dependent regulation of calcium transport capacity, but it remains to be established whether this is through changes in gene expression or direct regulation of transporter activity. However, the expression of the Arabidopsis vacuolar H^+/Ca^{2+} antiporter, *AtCAX1*, is stimulated by increased Ca^{2+} supply (Hirschi, 2001).

The inability of rubidium to distribute in the same way as potassium suggests that rubidium may be a poor tracer for potassium in citrus leaves. Alternatively, it is possible that the mechanisms leading to cell-specific potassium distribution (Figs. 2 and 4) are different from those for calcium/strontium. Thus, rather than reflecting cell-specific transport properties, potassium/rubidium distribution might be the consequence of general and relatively similar accumulation by all cells followed by secondary redistribution processes (e.g. via symplastic transport) that give rise to the final potassium distributions observed. The strontium-induced redistribution of potassium to bundle sheath cells from palisade and spongy mesophyll cells (Fig. 6) indicates that potassium is mobile

between cells and so its initial accumulation in particular cells may not reflect its final location. We cannot rule out the possibility that symplastic transport also contributes to the observed distribution of strontium and calcium (compare with Cholewa and Peterson, 2004), but the simplest explanation for our data is that calcium and strontium move apoplastically and are taken up differentially by cells.

The lack of effect on strontium distribution when the adaxial surface was covered with Vaseline suggests that ions move to this part of the leaf by diffusion. The distance from a vascular bundle to the adaxial leaf surface is only approximately 100 μm (Fig. 1), so even if the diffusion coefficient for strontium or calcium in the cell walls is 100 times less than that in water, the time taken to diffuse this distance is only tens of seconds, making this mechanism feasible (Nobel, 1999). However, this does require a low concentration of strontium/calcium to be maintained at the adaxial leaf surface. This is probably achieved by rapid accumulation in the palisade and crystal-containing idioblast cells. The large accumulation of strontium and calcium in the apoplast around epidermal and idioblast cells (e.g. Fig. 4) is possibly an artifact of the high strontium and calcium concentrations fed to the excised leaves, and might not occur at normal xylem calcium concentrations (0.3–16.5 mM, depending on the calcium concentration external to the root; White and Broadley, 2003). Treatment of the abaxial surface with Vaseline completely stopped delivery of strontium in the xylem, so no conclusions could be drawn about the relative importance of mass flow and diffusion for strontium transport in this transverse half of the leaf.

As far as we are aware, this is the first study in which calcium transport into a range of different cell types in intact leaves has been studied using a tracer in XRMA experiments. We believe the technique has great potential and could be adopted for a range of elements, including those where investigations have been limited by the lack of a suitable radioactive tracer to measure uptake (e.g. magnesium). By growing plants under conditions that give low cellular concentrations of a particular element, and then providing that element to excised leaves, it should be possible to determine the patterns of accumulation in different cells. Further, pulse-chase approaches could be used to study secondary redistribution processes that might occur after initial uptake into cells. The technique is relatively noninvasive and so has the potential to identify sites of high rates of uptake or redistribution that can then be subsequently investigated using cell-specific techniques such as ion-selective microelectrodes (Miller et al., 2001), single-cell sampling (Tomos and Leigh, 1999), patch clamp (Ward, 1997), uptake into isolated protoplasts (Dietz et al., 1992), or microarray gene expression analysis (Leonhardt et al., 2004). Such cell-based approaches have already been used to demonstrate differences in gene expression and components of signaling pathways between stomatal guard cells and mesophyll cells (Sutton et al., 2000; Leonhardt et al., 2004) and may be useful in resolving mechanisms underlying the intercellular compartmentation of calcium.

MATERIALS AND METHODS

Plant Material

Seeds of Narara rough lemon (*Citrus jambhiri* Lush.) were germinated in sterilized coarse river sand and irrigated with one-quarter-strength Aquasol (Hortico, Homebush, Australia) and Sequestrene 138 Fe (Syngenta Crop Protection, Pendle Hill, Australia). After 3 months, individual seedlings were transplanted to 4-L pots containing the same sand medium and with the same fertigation treatment. Plants were grown in a naturally lit glasshouse in Merbein. The maximum/minimum air temperatures were 29°C to 24°C (day)/18°C to 16°C (night), respectively. At 6 months, seedlings were irrigated daily with a nutrient solution containing 2.5 mM $Ca(NO_3)_2$, 2.5 mM KNO_3, 1 mM $MgSO_4$, 0.5 mM KH_2PO_4, and micronutrients according to Hoagland and Arnon (1938), except that Fe was added as 0.1 mM FeNaEDTA. This is referred to as unamended nutrient solution. After 1 month, this was replaced for some of the plants by a similar solution containing 50 mM KCl, which decreased the calcium concentration in leaf cells (low-calcium growth conditions). An automatic watering system applied the solutions twice daily. Excess solution was applied on each occasion to prevent the accumulation of salts in the sand. Plants were irrigated with the treatment solutions for 3 to 4 months before leaves were used in XRMA experiments. One to 2 months before these experiments, plants were trimmed back to a single shoot to induce growth flushes that ensured leaves used in the experiment had developed under the nutrient treatment and were of approximately equal age. For the experiment in Table I, leaves of different ages were obtained by selecting a recently emerged, almost fully expanded leaf and another from the 17th node distal to that leaf. Exact ages were not recorded.

Strontium and Rubidium Uptake Experiments

Leaves were excised under water at the point of attachment of the petiole to the stem, and the petiole was inserted through a hole in the cap of a 70-mL polystyrene vial so it was fully immersed in the uptake solution (composition in figure and table legends). Leaves were allowed to take up the solution for 4 or 24 h in a glasshouse in partial sunlight (photosynthetically active radiation of approximately 500 μmol m^{-2} s^{-1}) and with day and night temperatures of 25°C and 20°C, respectively. In some experiments, one or the other of the leaf surfaces was covered with a thin layer of Vaseline to examine the consequences of decreasing water loss. This was carefully removed with a soft tissue prior to preparation for XRMA. Vaseline application is a nontoxic method for stopping water loss from leaves and other plant tissues (McIntyre, 1994; Manter et al., 2000).

Cryoscanning Electron Microscopy and XRMA

Leaves were washed by dipping them briefly in deionized water and 2 mm × 5 mm segments of tissue were excised from the middle section of the leaf and mounted on aluminum stubs. (Preliminary labeling experiments showed that strontium distribution was highest and most uniform in the middle of the leaf.) When two treatments were being compared, leaf segments from each treatment were mounted in the same stub and their position relative to a small groove cut in the stub was noted to aid subsequent identification. The leaf segments were surrounded by a small volume of water and frozen in liquid N_2 or N_2 slush. The frozen, fully hydrated specimen was transferred under liquid N_2 into a Balzers SCU 102 preparation chamber (Balzers Union Aktiengesellschaft, Furstentum, Liechtenstein). The specimen (at −105°C) was cryoplaned using a stainless steel microtome blade cooled to approximately −50°C. The samples were etched at −86°C for 4 min under the control of a Digitronik temperature programmer (Yamatake-Honeywell, Tokyo) capable of outputting reproducible temperature profiles, thus ensuring that all samples received the same etching treatment. Samples were recooled to −130°C and sputter coated with gold.

The coated specimens were analyzed in a Philips 500 scanning electron microscope (Philips Electron Optics, Eidenhoven, The Netherlands) fitted with an EDAX energy-dispersive x-ray detector (EDAX International,

Mahwah, NJ) and a Link AN10000 x-ray microanalyzer (Oxford Instruments Microanalysis Group, High Wycombe, UK). XRMA spectra from 0 to 10 keV were recorded at an accelerating voltage of 12 kV, using a beam diameter of approximately 0.4 μm (about 1,500 cps) and a data collection time of 100 live s. Spectra were analyzed by the proprietary AN10000 ZAF-P/B software. Results are reported as (p − b)/b ratios, which is a semiquantitative proxy for element concentration (Sigee, 1993). Conversion of (p − b)/b ratios to element concentrations was not done because it requires control of a number of parameters for all specimens, including specimen height on the stub, rate and duration of etching, thickness of the gold coating, and beam current. We considered semiquantitative analysis was appropriate for this study, allowing more samples to be processed but still giving good indications of differences between cell types. A typical (p − b)/b ratio for a 333 mM calcium solution in our XRMA system was 0.8, and relative (p − b)/b ratios for potassium versus chlorine, calcium versus chlorine, and strontium versus chlorine were 1.3, 1.5, and 1.1, respectively. Values of (p − b)/b ratios in Figure 5, but not in other figures and tables, were adjusted for the different sensitivities to calcium and strontium. Paired analysis of leaf samples in the same stub provided quantitative comparisons between treatments. To measure the relative distributions of strontium to each leaf surface, intact pieces of leaf were frozen as above, mounted on a stub, coated with gold, but not cryoplaned. The electron beam was focused on the appropriate surface of the leaf and the (p − b)/b for strontium was measured using an accelerating voltage of 25 kV to ensure adequate penetration to the underlying cells. Elemental distribution maps were collected in real-time mode. First, a secondary electron image of the specimen was stored direct to disc at a resolution of 512 × 512 pixels. Then multiple scans were made of the same region of the specimen to collect the maps at a resolution of 128 × 128 pixels. X-ray counts were typically in the range from 1,000 to 1,500 cps and the pixel dwell time was 10 ms.

Light Microscopy

Small leaf slices were fixed in a 5:5:45:45 (v/v) mixture of formalin:propionic acid:ethanol:water at room temperature for 24 h. The fixed samples were dehydrated in an alcohol series comprising methoxyethanol, ethanol, propanol, and butanol. Samples were infiltrated with glycol methacrylate and polymerized for 2 d at 60°C. Five-micrometer-thick sections were cut with a Reichert-Jung 2040 microtome (Leica, Wetzlar, Germany) and examined with an Olympus BX51 microscope (Olympus Optical,Tokyo).

Statistical Analysis

All statistical analyses were carried out using Genstat 5, release 4.1 (Lawes Agricultural Trust, Rothamsted Research, Harpenden, UK). Data sets were analyzed by either ANOVA or two-way restricted maximum likelihood. Data were graphed with SigmaPlot 2000 (SPSS, Chicago, IL).

Terminology

XRMA measures elements and does not allow inferences to be made about the ions or chemical species present. Therefore, results from these analyses are reported using the appropriate symbol for the elements (potassium, calcium, strontium, chlorine, etc). Where underlying physiological processes that are known to involve ions are discussed, then the symbols for the ions are used (e.g. K^+, Ca^{2+}, Sr^{2+}, Cl^-, etc).

Received April 30, 2004; returned for revision June 5, 2004; accepted June 7, 2004.

LITERATURE CITED

Atkinson CJ (1991) The flux and distribution of xylem sap calcium to adaxial and abaxial epidermal tissue in relation to stomatal behaviour. J Exp Bot **42:** 987–993

Boursier P, Läuchli A (1989) Mechanisms of chloride partitioning in the leaves of salt-stressed *Sorghum bicolor* L. Physiol Plant **77:** 537–544

Broadley MR, Bowen HC, Cotterill HL, Hammond JP, Meacham MC, Mead A, White PJ (2003) Variation in the shoot calcium content of angiosperms. J Exp Bot **54:** 1431–1446

Canny MJ (1990) What becomes of the transpiration stream? New Phytol **114:** 341–368

Cholewa E, Peterson CA (2004) Evidence for symplastic involvement in the radial movement of calcium in onion roots. Plant Physiol **134:** 1793–1802

De Silva DLR, Hetherington AM, Mansfield TA (1985) Synergism between calcium ions and abscisic acid preventing stomatal opening. New Phytol **100:** 473–482

De Silva DLR, Hetherington AM, Mansfield TA (1996) Where does all the calcium go? Evidence of an important regulatory role for trichomes in two calcicoles. Plant Cell Environ **19:** 880–886

De Silva DLR, Mansfield TA (1994) The stomatal physiology of calcicoles in relation to calcium delivered in the xylem sap. Proc R Soc Lond B Biol Sci **257:** 81–85

Dietz K-J, Schramm M, Lang B, Lanzl-Schramm A, Dürr C, Martinoia E (1992) Characterization of the epidermis from barley primary leaves. II. The role of the epidermis in ion compartmentation. Planta **187:** 431–437

Esau K (1977) Anatomy of Seed Plants, Ed 2. John Wiley and Sons, NY

Franceschi VR, Schueren AM (1986) Incorporation of strontium into plant calcium-oxalate crystals. Protoplasma **130:** 199–205

Fricke W, Leigh RA, Tomos AD (1994) Concentrations of inorganic and organic solutes in extracts from individual epidermal, mesophyll and bundle-sheath cells of barley leaves. Planta **192:** 310–316

Gierth M, Stelzer R, Lehmann H (1998) Endodermal Ca and Sr partitioning in needles of the European Larch (*Larix decidua* (L.) Mill.). J Plant Physiol **152:** 25–30

Hirschi K (2001) Vacuolar H^+/Ca^{2+} transport: Who's directing the traffic? Trends Plant Sci **6:** 100–104

Hoagland DR, Arnon DI (1938) The water-culture method for growing plants without soil. Circular 347, University of California, College of Agriculture, Berkeley, CA

Hodson MJ, Sangster AG (1988) Observations on the distribution of mineral elements in the leaf of wheat (*Triticum aestivum* L.), with particular reference to silicon. Ann Bot (Lond) **62:** 463–471

Karley AJ, Leigh RA, Sanders D (2000a) Differential ion accumulation and ion fluxes in the mesophyll and epidermis of barley. Plant Physiol **122:** 835–844

Karley AJ, Leigh RA, Sanders D (2000b) Where do all the ions go? The cellular basis of differential ion accumulation in leaf cells. Trends Plant Sci **5:** 465–470

Kim TW, Heinrich G (1994) Calmodulin stimulation of Sr^+/nH^+ antiport in vacuoles of red beet (*Beta vulgaris*) storage tissue. Biol Plant (Prague) **36:** S-1525

Kim TW, Heinrich G (1995) Use of a laser microprobe mass analyzer for detection of strontium incorporation in oxalate-crystals of *Beta vulgaris* leaf. J Plant Physiol **146:** 217–221

Küpper H, Lombi E, Zhao F, McGrath SP (2000) Cellular compartmentation of cadmium and zinc in relation to other elements in the hyperaccumulator *Arabidopsis halleri.* Planta **212:** 75–84

Küpper H, Lombi E, Zhao F, Wieshammer G, McGrath SP (2001) Cellular compartmentation of nickel in the hyperaccumulators *Alyssum lesbiacum*, *Alyssum bertolonii* and *Thlaspi goesingense.* J Exp Bot **52:** 2291–2300

Leigh RA (2001) Potassium homeostasis and membrane transport. J Plant Nutr Soil Sci **164:** 193–198

Leigh RA, Chater M, Storey R, Johnston AE (1986) Accumulation and subcellular distribution of cations in relation to the growth of potassium-deficient barley. Plant Cell Environ **9:** 595–604

Leigh RA, Storey R (1993) Intercellular compartmentation of ions in barley leaves in relation to potassium nutrition and salinity. J Exp Bot **44:** 755–762

Leigh RA, Tomos AD (1993) Ion distribution in cereal leaves: pathways and mechanisms. Philos Trans R Soc Lond B Biol Sci **341:** 75–86

Leonhardt N, Kwak JM, Robert N, Leonhardt G, Schroeder JI (2004) Miroarray expression analyses of Arabidopsis guard cells and isolation of a recessive abscisic acid hypersensitive protein phosphatase 2C mutant. Plant Cell **16:** 596–615

Levy-Lior A, Weiner S, Addadi L (2003) Achiral calcium-oxalate crystals with chiral morphology from the leaves of some *Solanaceae* plants. Helv Chim Acta **86:** 4007–4017

Lombi E, Zhao F, Fuhrmann M, Ma LQ, McGrath SP (2002) Arsenic distribution and speciation in the fronds of the hyperaccumulator *Pteris vittata.* New Phytol **156:** 195–203

Manter DK, Bond BJ, Kavanagh KL, Rosso PH, Filip GM (2000) Pseudotheca of Swiss needle cast fungus, *Phaeocryptopus gaeumannii*, physically block stomata of Douglas fir, reducing CO_2 assimilation. New Phytol **148:** 481–491

McIntyre GI (1994) The role of transpiration in phototropism of the *Avena* coleoptile: evidence of stomatal control of the phototropic response. Aust J Plant Physiol **21:** 359–375

Miller AJ, Cookson SJ, Smith SJ, Wells DM (2001) The use of microelectrodes to investigate compartmentation and the transport of metabolized inorganic ions in plants. J Exp Bot **52:** 541–549

Nelson DP, Pan WL, Franceschi VR (1990) Xylem and phloem transport of mineral nutrients from *Solanum tuberosum* roots. J Exp Bot **41:** 1143–1148

Nobel PS (1999) Physiochemical and Environmental Plant Physiology, Ed 2. Academic Press, NY

Robinson JB, Treeby MT, Stephenson RA (1997) Fruits, vines and nuts. *In* DJ Reuter, JB Robinson, eds, Plant Analysis: An Interpretation Manual, Ed 2. CSIRO Publishing, Collingwood, Australia, pp 349–382

Schneider H (1968) The anatomy of citrus. *In* W Reuther, LD Batchelor, HJ Webber, eds, The Citrus Industry, Vol 2, Anatomy, Physiology, Genetics and Reproduction. University of California Press, Berkeley, CA, pp 1–85

Sigee DC (1993) X-Ray Microanalysis in Biology: Experimental Techniques and Applications. Cambridge University Press, Cambridge, UK

Storey R, Schachtman DP, Thomas MR (2003) Root structure and cellular chloride, sodium and potassium distribution in salinized grapevines. Plant Cell Environ **26:** 789–800

Sutton F, Paul SS, Wang X-Q, Assmann SM (2000) Distinct abscisic acid signaling pathways for modulation of guard cell versus mesophyll cell potassium channels revealed by expression studies in *Xenopus laevis* oocytes. Plant Physiol **124:** 223–230

Taylor BK, Dimsey RT (1993) Rootstock and scion effects on the leaf nutrient composition of citrus trees. Aust J Exp Agric **33:** 363–371

Tomos AD, Leigh RA (1999) The pressure probe: a versatile tool in plant cell physiology. Annu Rev Plant Physiol Plant Mol Biol **50:** 447–472

Treeby MT, van Steveninck RFM, Devries HM (1987) Quantitative estimates of phosphorus concentrations within *Lupinus luteus* leaflets by means of electron probe x-ray microanalysis. Plant Physiol **85:** 331–334

Ward JM (1997) Patch-clamping and other molecular approaches for the study of plasma membrane transporters demystified. Plant Physiol **114:** 1151–1159

White PJ (2001) The pathways of calcium movement to the xylem. J Exp Bot **52:** 891–899

White PJ, Bowen HC, Demidchik V, Nichols C, Davies JM (2002) Genes for calcium-permeable channels in the plasma membrane of plant root cells. Biochim Biophys Acta **1564:** 299–309

White PJ, Broadley MR (2003) Calcium in plants. Ann Bot (Lond) **92:** 487–511

Williams ML, Thomas BJ, Farrar JF, Pollock CJ (1993) Visualizing the distribution of elements within barley leaves by energy-dispersive x-ray image maps (EDX maps). New Phytol **125:** 367–372